Carbohydrate Polymer Technologies and Applications 8 (2024) 100543

Contents lists available at ScienceDirect

Carbohydrate Polymer Technologies and Applications

journal homepage: www.sciencedirect.com/journal/carbohydrate-polymer-technologies-and-applications

Mitochondria embedded in degalactosylated xyloglucan hydrogels to improve mitochondrial transplantation

Pasquale Picone [a], Emanuela Muscolino [b,c,*], Antonella Girgenti [a], Maria Testa [c], Daniela Giacomazza [b], Clelia Dispenza [b,c,1], Domenico Nuzzo [a,1]

[a] Consiglio Nazionale delle Ricerche, Istituto per la Ricerca e l'Innovazione Biomedica, Via U. La Malfa 153, Palermo 90146, Italy
[b] Consiglio Nazionale delle Ricerche, Istituto di Biofisica, Via U. La Malfa 153, Palermo 90146, Italy
[c] Dipartimento di Ingegneria, Università degli Studi di Palermo, Viale delle Scienze, Bldg 6, Palermo 90128, Italy

ARTICLE INFO

Keywords:
Mitochondria
Hydrogel delivery device
Mitochondrial transplantation
Degalactosylated xyloglucan
Heart injection
Hydrogel injection

ABSTRACT

Mitochondria are the major source of intracellular adenosine triphosphate (ATP) and play an essential role in a plethora of physiological functions, including regulating metabolism and maintaining cellular homeostasis. Mitochondrial dysfunction is associated with the onset of several cardiovascular diseases and, although several approaches currently exist to counteract it, no treatment using mitochondria as a therapeutic target exists to date. Recently, mitochondrial transplantation (MT) has been identified as a potential therapy that leads to increased ATP production, reduced oxidative stress, and improved bioenergetics. MT involves the replacement of damaged mitochondria, following injury or diseases.

With MT, mitochondria must survive an inhospitable extracellular environment often characterized by oxidizing agents due to pathological and/or inflammatory conditions. Furthermore, only a small percentage of the injected mitochondria reaches the target site due to dispersion throughout the body.

In this work, an MT strategy involving degalactosylated xyloglucan hydrogel encapsulating mitochondria, to overcome MT problems and improve its efficiency, is illustrated for the treatment of cardiovascular damage. The presence of the hydrogel presents the following advantages: improves the health of mitochondria; plays a protective role towards mitochondria from the extracellular environment and oxidative stress; allows for sustained release of viable mitochondria and local transfer into host cells.

Hypothesis

Incorporating mitochondria into a degalactosylated xyloglucan hydrogel will enhance mitochondrial transplantation for cardiovascular damage care maintaining viability and preventing oxidative stress.

1. Introduction

Mitochondria are important intracellular organelles present in all mammalian cells, except for mature red blood cells. They play a key role in energy production and several other important cellular functions, such as heat regulation, calcium homeostasis, biogenesis and iron-sulfur protein assembly, control of apoptosis, reactive oxygen species (ROS) production, cell survival, and proliferation, production of metabolites and coordination of metabolic pathways (Loureiro et al., 2017; McCully et al., 2016; Rüb et al., 2017; Salimi et al., 2015, 2017).

Mitochondrial dysfunction can be observed in a range of diseases, such as cardiovascular and neurodegenerative diseases, ischemia, diabetes, skeletal muscle and liver disorders, aging, and cancer progression (Belosludtsev et al., 2020; X. Chen et al., 2023; Ma et al., 2020; McCully et al., 2016; Picone et al., 2014; Poznyak et al., 2020; Wang et al., 2020; Zhang et al., 2008). In pathological conditions, impaired mitochondrial electron transport chain activity increases reactive oxygen species (ROS) production, leading to mitochondrial-driven injuries (Pecora et al., 2022). Mitochondrial oxidative stress contributes to cell damage by inducing lipid peroxidation, protein oxidation, and DNA modifications.

* Corresponding author.
E-mail address: emanuela.muscolino@unipa.it (E. Muscolino).
[1] This authors have contributed equally to this work.

https://doi.org/10.1016/j.carpta.2024.100543

Available online 7 July 2024

In human cells, mitochondria may not only differ from cell to cell in terms of number, but also in size, shape, distribution, and characteristics. Moreover, they can change and adapt depending on the physiological or pathological conditions of the cell (Bragoszewski et al., 2017). In tissues with a high energy demand, such as the heart, one-third of the cell volume is occupied by mitochondria (Protasoni & Zeviani, 2021). In the event of mitochondrial dysfunction, the heart is like an engine without fuel. Likewise, the Central Nervous System (CNS) is rich in mitochondria, so the production of high levels of metabolites and ROS can be expected (Di Carlo et al., 2012; Picone et al., 2020). Supporting this notion, mitochondrial dysfunction has been reported in several neurodegenerative diseases such as Alzheimer, Multiple Sclerosis (MS), Amyotrophic Lateral Sclerosis (ALS), Parkinson's disease (PD), and other nervous system diseases (Bonafede & Mariotti, 2017; Giannoccaro et al., 2017; Kuo et al., 2017; Picone et al., 2014, 2016; Picone & Nuzzo, 2022; Shaki et al., 2017; Zhao et al., 2022).

Recently, the term "mitochondrial transplantation" (MT) has opened a novel horizon for many diseases (Emani et al., 2017; McCully et al., 2016). MT is a potential new treatment consisting of mitochondrial transfer, which aims to replace mitochondria in cells with damaged mitochondria, thus arresting mitochondrial dysfunction in injury and disease states. It has been shown that when neurons are damaged by an ischemic stroke, astrocytes generously deliver their healthy mitochondria to neurons, via vesicles containing them to induce neuroprotection. Replacing damaged mitochondria with healthy ones in cells improves energy production, reverses excessive ROS production and restores mitochondrial functions (Lu et al., 2017; Paliwal et al., 2018).

Due to their small size (~ 1 μm), mitochondria can be delivered intravenously. They are not incorporated into red blood cells and do not interfere with oxygen transport (Shi et al., 2017). During mitochondrial isolation, it is essential to satisfy the criteria of good manufacturing practice (GMP). The number, purity, form, viability, and function of organelles must be controlled as part of the quality assurance process. Their viability and function can be analyzed by fluorescent probes (MitoTracker, JC1), and measurement of oxygen consumption and ATP levels (Preble et al., 2014).

McCully and colleagues employed MT as a therapeutic approach to treat cardiac ischemia both in animal models and in patients (McCully et al., 2017). They injected autologous functional mitochondria into ischemic pig hearts, isolating healthy mitochondria from the pectoralis major muscle. Mitochondria were injected into eight risk areas. The results showed that the infarct size in the group that received mitochondria was significantly smaller (Kaza et al., 2017).

Masuzawa et al. (2013) extracted functional mitochondria of non-ischemic skeletal muscles and injected them into the ischemic area of a rabbit model. After 28 days, the results obtained with the experimental group that received mitochondria showed an effective reduction in necrosis and apoptosis of cardiomyocytes and a development of cardiac function (Masuzawa et al., 2013). In pediatric patients with cardiac ischemia (five children, age from 2 days to 2 years) mitochondria were extracted from two different samples obtained from the rectus abdominis and injected, using a tuberculin syringe, directly into the ischemic areas. After the transplant, none of the patients had bleeding or arrhythmia due to the injection. In four of the patients, cardiac functions improved according to echocardiographic findings, and extracorporeal membrane oxygenation (ECMO) support was no longer required. (Emani et al., 2017).

Although MT has been referred to as a "magical" cure, since mitochondria, harvested from healthy tissues and injected in damaged ones, seem to restore ATP and mitochondrial functions (Bertero et al., 2018), it has limitations and challenges that must be overcome.

Mitochondria must survive the transition from an intracellular to extracellular environment, with high calcium concentrations, and cross the cellular and bodily barriers. Immunogenicity and activation of immune response is one of the important aspects of the MT. McCully and collaborators demonstrated that autologous MT does not induce any immune response in various animal models (McCully et al., 2017). However, in the case of congenital mitochondrial disease, autologous MT may not be suitable, because mitochondria in other tissues may be dysfunctional.

Studies on the immune response in mice after single or multiple intraperitoneal injections of allogeneic mitochondria found that serum cytokine levels did not increase after autologous or allogeneic MT (Ramirez-Barbieri et al., 2019). In contrast, Brennan and collaborators demonstrated that the heart early develops a marked rejection response to a single injection of allogeneic mitochondria with elevated secretion of inflammatory cytokines and chemokines (Lin et al., 2019). Long-term safety and potential side effects of mitochondrial transplantation require thorough investigation, such as abnormal cell function or tumorigenesis.

Moreover, data report that only a small percentage (≤6 %) of injected mitochondria can actually reach brain cells (Gollihue et al., 2017, 2018), and only about 10 % are taken up by cardiomyocytes (Emani et al., 2017), while the majority of the injected ones are dispersed to other body districts. This is indeed a limitation of this therapeutic strategy and requires the development of methods that can improve the stability of mitochondria and prevent their dispersion. Recently, to improve mitochondrial release in neuronal cells, synaptosomes have been proposed as vesicles for MT (Picone et al., 2021). One possibility is also incorporating these organelles into injectable hydrogels. The polysaccharide dextran has been proposed to improve stabilization without affecting mitochondria activity (Wu et al., 2018). Tethering of dextran on the mitochondrial surface has been achieved using triphenylphosphonium bromide (TPP), a molecule that has a specific mitochondrial tropism. Further improvement in organelle transplantation has been achieved by linking dextran-covered mitochondria to the cell-penetrating peptide (CPP) TAT, for specific cellular targets (Wu et al., 2018). Patel and co-workers developed a heat-gelling, erodible hydrogel to protect isolated mitochondria from the extracellular environment and deliver them to the injured spinal cord, in a controlled way. The authors evaluated the ability of these hydrogels to release and maintain the integrity of isolated mitochondria. They found that 70 % of mitochondria were released from the hydrogel within 20 min at 37 °C and that the respiratory capacity of mitochondria released from the hydrogel in 60 min was greater than that recorded for free mitochondria. Furthermore, hydrogel allowed for their local diffusion and incorporation into host cells (Patel et al., 2022).

In this work, an in-situ forming hydrogel based on partially degalactosylated xyloglucan (dXG) is used to incorporate mitochondria and support their successful transplantation. Xyloglucan (XG), derived from tamarind seed, is a non-ionic, water-soluble polysaccharide, composed of a β-(1,4)-d-glucan backbone, partially substituted by α-(1,6)-linked xylose unit, that can be partially β-d-galactosylated at O-2. XG is commercially available, non-toxic, biodegradable (D. Chen et al., 2012; Miyazaki et al., 2001), and FDA-approved as a food additive (Dea, 1989). In drug delivery, xyloglucan provides sustained release profiles, encapsulating drugs and protecting them from premature degradation. The suitability of XG in tissue engineering is further supported by its ability to interact with biological tissues. Xyloglucan hydrogels can adhere to various tissues, providing a supportive environment for cell attachment, proliferation, and differentiation. Studies have demonstrated its effectiveness in promoting cell viability and tissue integration, which are critical factors for successful tissue engineering applications (Dutta et al., 2020). When partially degalactosylated (dXG) and dispersed into aqueous media at relatively low concentration and low temperature, quickly sets at body temperature into soft, conformable, and durable hydrogels without any chemicals or additives (Han et al., 2020; Shirakawa et al., 1998; Todaro et al., 2015) so it can be injected for biomedical applications and form hydrogel in situ. Both XG and dXG can be conveniently tailored by radiation-induced modification of the molecular weight distribution modifying their chemical physical properties for different scopes (Muscolino et al., 2024; Todaro et al., 2016). dXG has already been studied as an in-situ forming scaffold for cartilage

reconstruction (Dispenza et al., 2017), and as an artificial niche of stem cells, showing the ability to preserve cell viability and stemness (Toia et al., 2020) or, when formulated with *ad hoc* media, to stimulate stem cell differentiation in osteocytes or chondroblasts (Muscolino et al., 2021). Here we investigated whether a dXG gel, which is formed in situ at body temperature from an easily injectable liquid solution, can incorporate mitochondria, preventing their dispersion and allowing their gradual release. It was also evaluated whether the mitochondria incorporated into the hydrogel can be protected from oxidative stress potentially present in the extracellular environment. In addition, Lim and coworkers demonstrated that tamarind-derived xyloglucan would show myocardial protection by inhibiting apoptosis and improving energy metabolism (Lim & Lee, 2017), which could be an additional advantage for the use of xyloglucan scaffolds.

2. Materials and methods

2.1. Hydrogel preparation

Partially degalactosylated tamarind seed xyloglucan (dXG) was kindly provided by MP GOKYO FOOD & CHEMICAL CO., LTD. Therefore, Xyloglucan (XG), composed of a β-(1,4)-d-glucan backbone, partially substituted by α-(1,6)-linked xylose unit, again partially substituted by β-d-galactosylatose at O-2, was provided in this case already degalactosylated, with a degalactosylation degree of 45 % and purity > 95 %. The apparent molecular weights values (M_{app}) were obtained from GPC, calibrated with Pullulans standards, performed with the Agilent 1260 Infinity HPLC, coupled to a refraction index (RI) detector, using two Shodex SB HQ columns (804 and 806) connected in series on sample prepared as 0.1 %w aqueous dispersions, filtered through 0.80-micron membrane syringe filters prior to analysis to remove contaminants, and eluted with 0.02 %w NaN_3 solution at 0.6 ml/min. Results are presented in Fig. S1 of supplementary material. Weight average M_{app}: 3.99×10^6 Da; number average M_{app}: 1.59×10^6 Da; Đ: 2.50.

For hydrogel preparation, Complete Dulbecco's Modified Eagle's Medium and F12 (DMEM/F12; 1:1) was used, supplemented with 10 % fetal bovine serum (FBS) (GIBCO Invitrogen, Milan, Italy), 100 U/mL penicillin and 100 U/mL streptomycin, and 2 mM l-glutamine. The medium was added to dXG powder to reach a 6 %w concentration, and stirred for about 30 min at 5 °C until a homogenous dispersion was obtained.

The 6 %w dXG dispersion was then used to prepare the final hydrogels by gently mixing it in a 2:1 ratio with mitochondria culture medium with or without mitochondria, to reach a final concentration of 4 %w.

The analogous system with water was prepared by adding water to dXG powder to reach a 4 %w concentration and stirred for about 30 min at 5 °C until a homogenous dispersion was obtained.

Each system is named hereafter as dXG4-X, where 4 indicates the final polymer concentration in weight percentage and X is a letter referring to the swelling/culture medium that has been mixed with the dXG powder. In particular, W stands for water, and D for the modified DMEM/F12. When mitochondria were added to the hydrogel, the word "Mito" is added to the code.

2.2. Rheological measurements

Dynamic mechanical spectra were determined using a stress-controlled Rheometer AR G2 (TA Instruments). The geometry used was a PIK anti-slippery plate of 20 mm diameter and the gap was set in the range 500–1000 μm.

Strain sweep measurements were performed to explore the extension of the linear viscoelastic range, at 1 Hz, and identify the optimum strain conditions for the subsequent frequency sweep tests.

The gelation behavior was studied by performing oscillatory measurements in time sweep mode. Samples were prepared at 5 °C, then equilibrated to room temperature, placed on the rheometer plate at 37 °C and analysis started immediately to simulate the temperature steps of injection into the human body.

The plate temperature was kept at 37 °C via a built-in Peltier control for 1 h. The frequency was set at 1 Hz and the strain at 1.2×10^{-3}.

Frequency sweep measurements were also performed at a constant strain of 1.2×10^{-3} and in the 0.1 - 10 Hz frequency range. Known volumes of the formulations were either placed or injected on the bottom plate and the measurements started after 10 min of thermal and structural equilibration at the measurement temperature of 37.0 ± 0.1 °C.

2.3. Morphological analysis

Hydrogel microstructure was investigated using a Field Emission Scanning Electron Microscope (SEM) FEI Quanta 200 FEG at an accelerating voltage of 10 kV. The hydrogels were frozen in liquid nitrogen, freeze-dried, mounted on aluminum stubs, and gold coated by JFC-1300 gold coater (JEOL) for 120 s at 30 mA before scanning.

2.4. Cell culture

SH-SY5Y cells, generously provided by Dr. Venera Cardile, University of Catania, Italy, were cultured in T75 tissue culture flasks. Complete Dulbecco's Modified Eagle's Medium and F12 (DMEM/F12; 1:1) was used, supplemented with 10 % fetal bovine serum (FBS) (GIBCO Invitrogen, Milan, Italy), 100 U/mL penicillin and 100 U/mL streptomycin, and 2 mM l-glutamine.

NIH 3T3 fibroblast cells were cultured with DMEM with 4.5 g/L glucose (Celbio srl, Milan, Italy) supplemented with 10 % Bovine Calf Serum (FCS) (Gibco-Invitrogen, Milan, Italy), 2 mm glutamine, 1 % penicillin, and 1 % streptomycin (50 mg mL−1). Cells were maintained in a humidified 5 % CO2 atmosphere at 37 ± 0.1 °C.

2.5. Mitochondrial isolation

Mitochondria fractions isolated from 2×10^7 cells of SH-SY5Y human neuroblastoma, were prepared using a Mitochondrial isolation kit (ThermoFischer, Italy) according to the manufacturer's instructions using buffers provided by the kit. Briefly, the cellular pellet was resuspended in of lysis buffer and homogenized on ice, centrifuged at 700 g for 10 min to remove cell debris. The supernatant was centrifuged at 12,000 g for 15 min at 4 °C and the mitochondrial pellet was washed twice by centrifugation at 12,000 g for 5 min and resuspended in the PBS. An aliquot was used to determine protein concentration (1 μg/μL) by the Bradford method. The amount of mitochondrial protein is usually accepted as a mitochondrial quantity, and an equal amount (50 μg) of mitochondrial protein was used for each measurement in all experiments.

2.6. Scanning electron microscopy of isolated mitochondria

The morphology of extracted mitochondria was observed through scanning electron microscopy (SEM) model Quanta 200F (FEI, Hillsboro, OR, USA) with the voltage set at 20 kV. Before analysis, mitochondria suspension was dipped on a cellulose membrane extracted from a commercial syringe filter with a pore size of 0.2 μm according to the manufacturer (CLS431222, Corning Inc., Corning, NY). The following common fixation protocol was applied (Lea & Hollenberg, 1989): the sample was washed with complete 1X phosphate-buffered saline (PBS) three times for 3 min each and fixed with 4 % glutaraldehyde for 30 min at 4 °C. Then, the sample was washed with 1X PBS and with increasing ethanol solution at room temperature (15 %, 30 %, 50 %, 75 %, 100 % v.v.) for dehydration; each wash was performed 3 times for 3 min. Finally, the sample was dried for 12 h at room temperature

under a fume hood. The sample was attached on an aluminum stub using an adhesive carbon tape and gold-sputtered for 90 s.

2.7. Mitochondrial viability

The mitochondrial membrane potential, as an index of mitochondrial viability, was measured by using a MitoProbe JC-1 Assay kit (Molecular Probes, Eugene, OR, USA). The mitochondria, resuspended in mitochondrial culture medium (DMEM/F12; 1:1 was used, supplemented with 10 % fetal bovine serum (FBS) (GIBCO Invitrogen, Milan, Italy), 100 U/mL penicillin and 100 U/mL streptomycin, and 2 mM l-glutamine) were incubated with 2 mM 5,5′,6,6′-tetrachloro-1,1′,3,3′-tetraethylbenzimidazolyl- carbocyanine iodide (JC-1) fluorescent dye for 30 min at 37 °C. Carbonyl cyanide 3-chlorophenylhydrazone (CCCP) (50 μM), a mitochondrial membrane potential disrupter, was used as a positive control. Fluorescence emission of red JC-1 aggregate inside the mitochondria, index of mitochondrial viability, was evaluated by fluorimeter (Multimode plate reader GloMax Discover – Promega, Madison, Wisconsin, USA) and fluorescence microscope, (Axio Scope 2 microscope; Zeiss) with 520 nm excitation laser and emission in the range 580–640 nm.

Mitochondrial viability was measured by MTS assay (Promega). MTS [3-(4,5- dimethylthiazol-2-yl)−5-(3carboxymethoxyphenyl)−2-(4-sulphophenyl)−2H-tetrazolium] was utilized according to the manufacturer's instructions. Mitochondria were seeded on 96-well plates and 20 μL of the MTS solution were added to each well, and incubated for 4 h at 37 °C, 5 % CO2. The absorbance was read at 490 nm on the Microplate reader Wallac Victor (Perkin Elmer).

2.8. Mitochondrial gel incorporation and impact of hydrogel on mitochondrial integrity

Specifically, 50 μg of JC-1 labeled mitochondria were transferred into 100 mg of hydrogel with a pipette and, with the help of a fine-tipped glass rod, were mixed gently to avoid bubble formation and obtain a homogeneous mixture.

To analyze the mitochondrial viability inside the hydrogel, the mitochondrion-loaded hydrogel was submitted to MTS assay. The sample was seeded on 96-well plates and 20 μL of the MTS solution were added to each well, and incubated for 4 h at 37 °C, 5 % CO2. The presence of the vital mitochondrial condition was visualized by the development of brown coloration and absorbance was read at 490 nm on the Microplate reader Wallac Victor (PerkinElmer). Hydrogel without mitochondria was used for background autofluorescence subtraction.

The MitoSOX was used for measurements of superoxide generated in the mitochondria following the mitochondrial oxidative state alterations. 100 μL of MitoSox reagent working solution (2uM) were added to the 96-well plate containing the gel-loaded mitochondria. Samples were incubated for 30 min at 37 °C and 5 % CO2. Then, they were twice gently washed in PBS buffer and analyzed by GloMax® Discover Multimode plate reader (Promega, Italy) at the excitation wavelength of 488 nm. The emission was recorded at the wavelength of 510 nm.

2.9. Analysis of mitochondrial release from hydrogel and cellular uptake

The hydrogel containing the JC-1 labeled mitochondria was inserted into the apical chamber of a transwell. Conversely, the acceptor chamber was filled with 0.5 mL of medium (DMEM/F12; 1:1 was used, supplemented with 10 % fetal bovine serum (FBS) (GIBCO Invitrogen, Milan, Italy), 100 U/mL penicillin and 100 U/mL streptomycin, and 2 mM l-glutamine), the whole was placed at 37 °C for a maximum of 24 h. At different times (1, 2, 4, 6, 20 and 24 h) the acceptor chamber medium was analyzed for the presence of JC-1 labeled mitochondria by fluorometric analysis.

To analyze the mitochondrial delivery to the cells, the mitochondria isolated from SY-5YSH were labeled with JC-1 Red probe and immediately loaded into the hydrogel. Subsequently, the gel with the loaded mitochondria was inserted into the apical chamber of a transwell where the SY-5YSH cells (1 × 105 cell/mL) were previously seeded in the basolateral chamber. After 24 h, the transwell was removed and the presence of red fluorescence in the cells was visualized by fluorescence microscopy.

2.10. Injectability

As part of the injectability assessment different types of measurements were carried out: (i) shear viscosity as a function of shear rate measurements (flow curves); (ii) rheological analysis in small-oscillatory conditions; and (iii) *ex-vivo* injection into the myocardial wall of swine hearts.

The flow curves of the dispersions formulated with DMEM/F12, with and without mitochondria, were obtained using the stress-controlled Rheometer AR G2, operating in rotational mode at the constant temperature of 25.0 ± 0.1 °C. Measurements were performed with the PIK anti-slippery of 20 mm diameter and a gap of 1000 μm.

The rheological analysis in small-oscillatory conditions was carried out on samples, with and without mitochondria, directly injected (needle: 18 G) on the rheometer plate at ca. 20 °C and let equilibrate at 37 °C for 10 min. Details on the experimental parameters are provided in Section 2.2.

The injection tests were performed by injecting 3–4 mL of the dXG dispersion into the myocardial wall of swine hearts purchased from the food market and conditioned at 37 °C, using a syringe (needle: 18 G) to visually assess gel spreading.

2.11. Mitochondrial protection from oxidative stress

Mitochondrial injury (o stress) was induced by hydrogen peroxide (H_2O_2). The JC1-labeled mitochondria, isolated or incorporated into the hydrogel, were treated with different concentrations of H_2O_2 (1, 10, 100 mM) and incubated at 37 °C and 5 % CO2 for 24 h. The fluorescent signal was determined at different times by GloMax® Discover Multimode plate reader (Promega, Italy) with 520-nm excitation laser and emission in the range 580–640 nm.

2.12. Statistical analysis

All experiments were repeated at least three times and each one was performed in triplicate. The results are presented as mean ± SD. A one-way ANOVA was performed, followed by Dunnett's post hoc test for analysis of significance. Results with a P-value $*P \leq 0.05$ and $**P \leq 0.02$ were considered statistically significant.

3. Results and discussion

3.1. Mitochondrial isolation and analysis

The mitochondria were isolated, in vitro, by a simple (few steps) and efficient protocol (less than 60 min) from SH-SY5H neuroblastoma cells (Fig. 1A). Different tissues can be used as a source of human mitochondria (Picone & Nuzzo, 2022); human neuronal cells were selected for this study to extract mitochondria as the central nervous system is one of the most mitochondria-rich tissues (Roushandeh et al., 2019). In particular, neuronal cells are rich in mitochondria and have high levels of cellular respiration (Roushandeh et al., 2019). .)Isolated mitochondria were visible under phase-contrast illumination (bright field) (Fig. 1B). To demonstrate the integrity of the extracted mitochondria, we performed a scanning electron microscope (SEM) measurement in which the isolated mitochondria did not evidence fractures or damage (Fig. 1C). Viability of isolated mitochondrial samples was confirmed by different techniques such as MTS and JC-1 tests. MTS assay is based on the presence of NAD(P)H-dependent dehydrogenase enzymes in

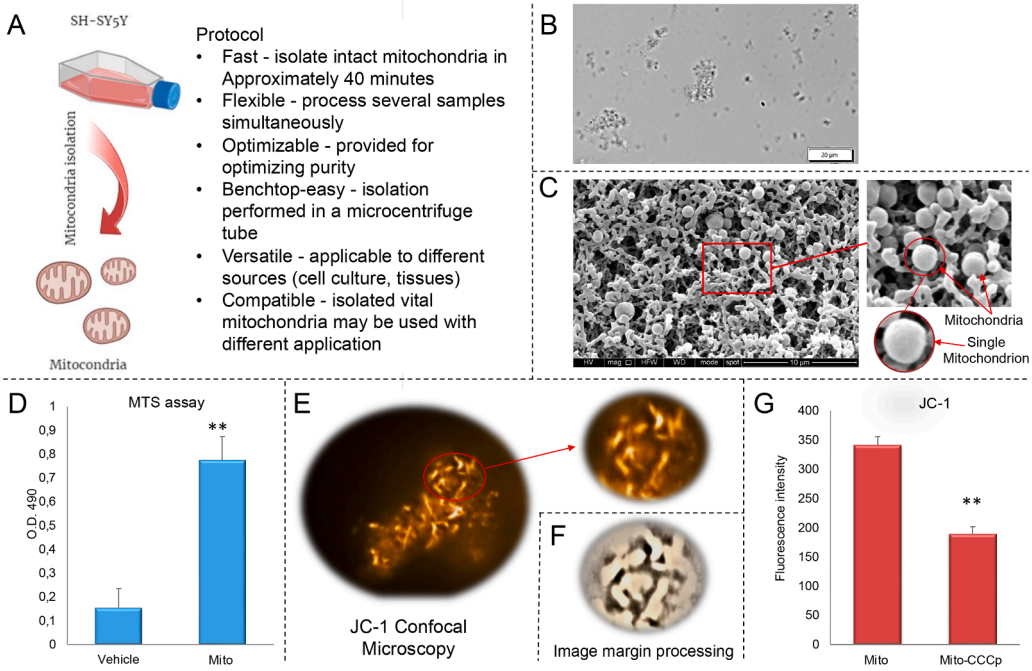

Fig. 1. Mitochondrial isolation and analysis. (A) Scheme and advantages of the mitochondria extraction protocol. (B) isolated mitochondria are shown under phase contrast illumination (bright field) and by SEM (C), in order to demonstrate the integrity of the extracted mitochondria. (D) MTS assay graph (measurement of mitochondrial metabolic activity) of isolated mitochondria and the vehicle (mitochondrial culture medium). (E) Confocal image of isolated mitochondria labeled with JC-1 probe, indicating the viability of isolated mitochondria. (F) Processing of the mitochondrial fluorescence image, where the contours are highlighted in order to confirm mitochondrial integrity. (G) Histogram of JC-1 fluorescence intensity of extracted mitochondria treated or not with CCCp indicating mitochondrial health. The results indicate that the isolated mitochondria are viable and metabolically active.

metabolically active mitochondria, therefore the MTS test can be considered a functional test for mitochondrial activity (Cha et al., 2012). In Fig. 1D, the high absorbance at 490 nm indicates the presence of vital mitochondria. Moreover, we used the fluorescent JC-1 probe, a membrane-permeant JC-1 dye, to monitor mitochondrial health. The dye JC-1 shows a membrane potential-dependent accumulation in the mitochondria. The monomeric form of the probe penetrates vital mitochondria where it aggregates, emitting intense red fluorescence. Consequently, if the mitochondrion is not viable and there is a depolarization of the mitochondrial membrane, a collapse of the red fluorescence occurs. By fluorimetry and confocal microscopy measurements, the extracted mitochondria showed high red fluorescence intensity (Fig. 1E, F). As a further check, when the membrane potential is deliberately compromised by the addition of CCCP, red JC-1 fluorescent intensity decreases, as indicated in the histogram of Fig. 1G. Moreover, by processing the fluorescence image, and highlighting the outline, the mitochondrial tubular morphology is shown (Fig. 1G). Morphology is an indication of healthy and viable mitochondria; in fact, viable mitochondria show tubular and branched mitochondrial networks, while damaged mitochondria are fragmented into short and swollen subunits with an oval shape. The success of MT depends on several factors such as the origin, the extraction time of the mitochondria (mitochondrial isolation must be performed in less than 2 h), the quality and stability of the mitochondria isolates, an appropriate release protocol (Picone & Nuzzo, 2022; Preble et al., 2014). Therefore, before MT, the size, shape, viability, and function of organelles must be subjected to quality control. Organelle viability can be analyzed using probes mitochondrial fluorescence (MitoTracker, JC1) and morphology (size, shape) and integrity using electron microscopy (Gollihue et al., 2017; Picone & Nuzzo, 2022; Roushandeh et al., 2019). The results, reported in Fig. 1, indicate that the protocol for mitochondrial isolation is very fast and that mitochondrial isolates are viable and metabolically active.

3.2. Hydrogel gelation behavior and mechanical properties

The process of partial degalactosylation of xyloglucan reduces the length of the grafted branches of the cellulosic backbone of the polymer and consequently decreases its hydrophilic character. The dXG disperses in water only at low temperatures (0 °C - 4 °C), where hydrogen bonds and dipole-dipole interactions with water are maximized. At higher temperatures, when the polymer-solvent interactions are weakened, the linear segments of the chains associate into ribbons, which in turn aggregate to form condensed domains. The hydrophobic interactions, which drive self-assembly, are counteracted by the repulsive hydration forces due to the presence of residual branches of a-(1, 6)-d-xylose linked to b-(1, 2)-d-galactose. At relatively high concentrations (above 1 %w) the association of polymeric segments belonging to different chains causes an increase of viscosity that progressively slows down the molecular dynamics and sets the system into a macroscopic gel, preventing phase separation (Sakakibara et al., 2017; Todaro et al., 2015). The concentration of polymer, the presence of other solvent or solute molecules can change the landscape of attractive and repulsive interactions, affect the gelation kinetics, and lead to a different network structure (Muscolino et al., 2021; Toia et al., 2020). These networks, when exposed to a large excess of aqueous solutions, slowly reorganize over time to reach a pseudo-equilibrium state, with insoluble fractions that can exceed 70 percent (Dispenza et al., 2017).

To understand the gelation behavior of the hydrogel that will host the mitochondria, time sweep tests in small oscillatory conditions, at constant strain and frequency, were performed at 37 °C starting from the dXG aqueous dispersion prepared at 4 °C with DMEM (dXG-D) and thermally equilibrated at 20 °C. The analogous system, formulated with only water (dXG-W), was prepared for comparison. From Fig. 2A it can be observed for both systems, that the storage modulus curve, G', is one order of magnitude higher than the loss modulus curve, G", already at time zero, revealing that the systems have become hydrogels already

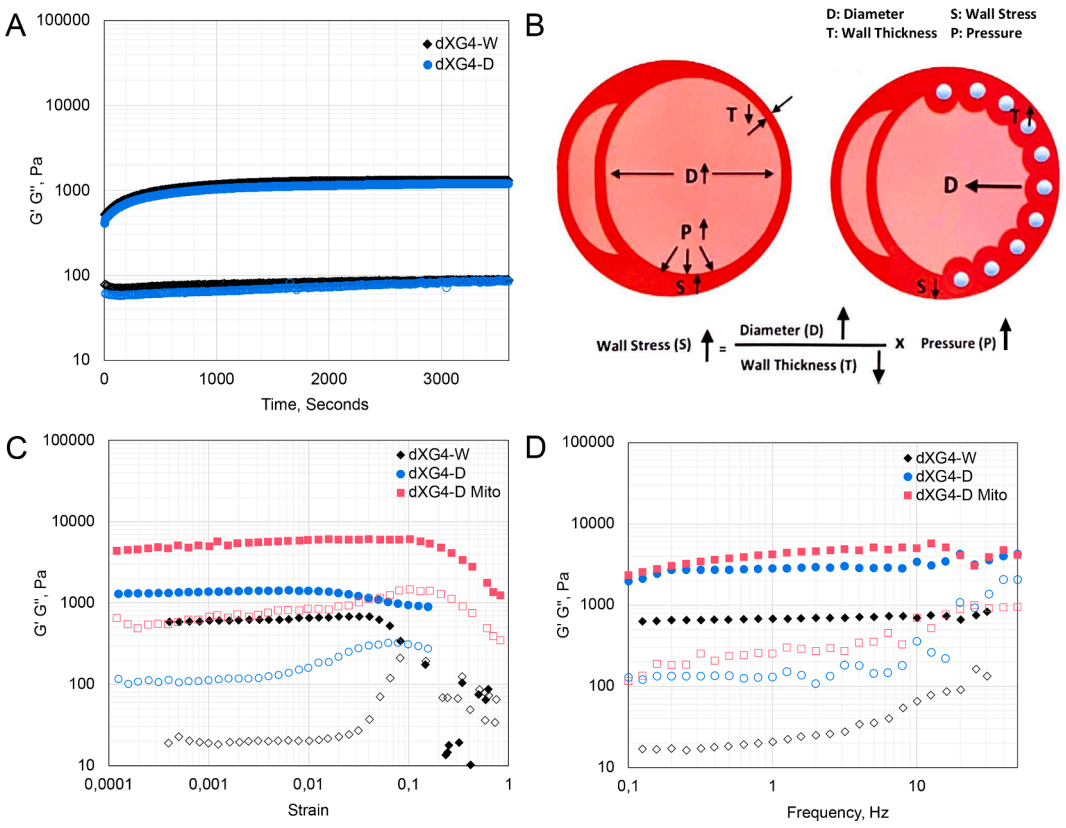

Fig. 2. Rheological Analysis. A) Storage modulus, G' (full dot), and loss modulus, G" (hollow dot), of dXG4-W and dXG4-D as a function of time. B) Schematization of left ventricular diameter, wall stress and pressure increase and wall thickness decrease after heart failure (left); and of the injection of hydrogel beads to remodel the wall thickness and chamber diameter (right). C) Storage modulus, G' (full dot), and loss modulus, G" (hollow dot), of dXG4-W and dXG4-D with and without mitochondria (Mito), as a function of strain; and D) as a function of frequency.

while equilibrating at 20 °C. At the very early stage of the test, the storage moduli increase, while the loss moduli decrease, and after about 1000s (ca. 15 min), both become invariant with time. These changes in G' and G" can be attributed to temperature equilibration and further structural rearrangements occurring at 37 °C that contribute to increased cross-linking density.

From the comparison of the rheological behavior of dXG4-W and dXG4-D in time sweep mode, one would conclude that the presence of the various solutes of the culture medium does not appreciably affect dXG gelation. The gelation process occurs with similar kinetics, with water and DMEM.

A more accurate characterization of the mechanical properties of the hydrogel can be performed in frequency sweep mode, at constant strain, after having carried out a strain sweep to identify the linear viscoelastic region and the shear values to be set for the frequency sweep analysis.

Fig. 2C-D shows the results of the strain and frequency sweep tests for dXG4-D with and without mitochondria at 37 °C, respectively. The G' and G" curves relative to dXG4-W are also reported, for comparison. Frequency sweep tests show for all systems G' values are well higher than the corresponding G" curves. From the mechanical spectra, we can appreciate significant differences among the three systems. dXG4-D has higher G' and G" curves than dXG4-W. It can be argued that, provided that sufficient time is given for the gelation process to occur (here 10 min at 37 °C) with no mechanical perturbations, the components present in the culture medium affect the polymeric network that is formed, thus, leading to a stronger hydrogel, as observed with similar systems (Muscolino et al., 2021; Toia et al., 2020). Identifying the specific cause of the observed effects is challenging, likely due to a combination of several factors. Amino acids, sugars, and salts present in the medium can significantly impact the gelation of polysaccharides through entropic effects (such as salting out or ion-mediated depletion forces) and by disrupting polymer-solvent hydrogen bonding interactions. These interactions can induce conformational changes in the polymer chains, leading to further intra- and intermolecular aggregation. All systems show a "frequency-dependence", especially in G", that is generally associated with heterogeneous networks, characterized by a range of relaxation times (Ditta et al., 2020; Giacomazza et al., 2018). The relatively high G' values of the hydrogel incorporating mitochondria suggest that this material may also play the role of a reinforcement of the cardiac wall if injected into the wall of an infarcted heart. As sketched in Fig. 2B, due to heart failure the left ventricular diameter increases and wall thickness decreases leading to increased wall stress and cardiac dysfunction; the injection of small hydrogel beads can alter the wall thickness and chamber diameter, thus reducing wall stress and inducing positive myocardial remodeling.

The rheological results can be further comprehended by observing the morphology of the systems shown in Fig. 3. dXG4-W 0 h shows an ordinary, random 3D network of interconnected pores with thin polymer walls. In some regions, shredded thin membranes are also evident. dXG4-D 0 h shows a more packed structure where thicker polymer lamellae are stacked and tightly interconnected which could account for the increased moduli observed in the mechanical analysis. Fig. 3B displays the morphologies of dXG4-D cross-sections at two different magnifications, as prepared (0 h) and after incubation at 37 °C for 6 h and 24 h. Over time (dXG4-D 6 h and 24 h), the polymer pores and lamellae appear to gradually open up, probably due to rearrangement of the network in the conditioning medium.

3.3. *Influence of the hydrogel on mitochondria viability*

To evaluate the impact of dXG4-D on the mitochondrial integrity, the mitochondria loaded into the hydrogel were subjected to JC-1 assay

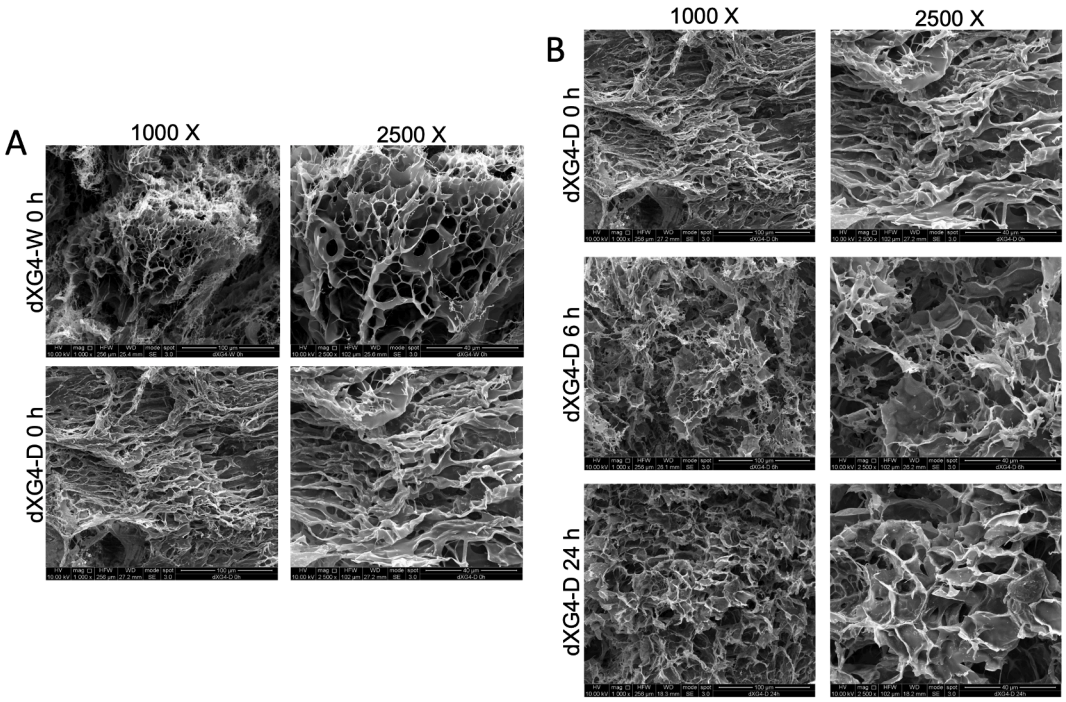

Fig. 3. Morphological analysis of as-prepared dXG4-W and dXG4-D and incubated dXG4-D. A) SEM micrographs (cross-sections) of dXG 4 %, prepared with water (dXG4-W) and DMEM/F12 (dXG4-D), as prepared (0 h) at two different magnifications (1000x and 2500x). B) SEM micrographs (cross-sections) of dXG 4 %, prepared with DMEM/F12 (dXG4-D), as prepared (0 h) and incubated for 6 h or 24 h at 37 °C.

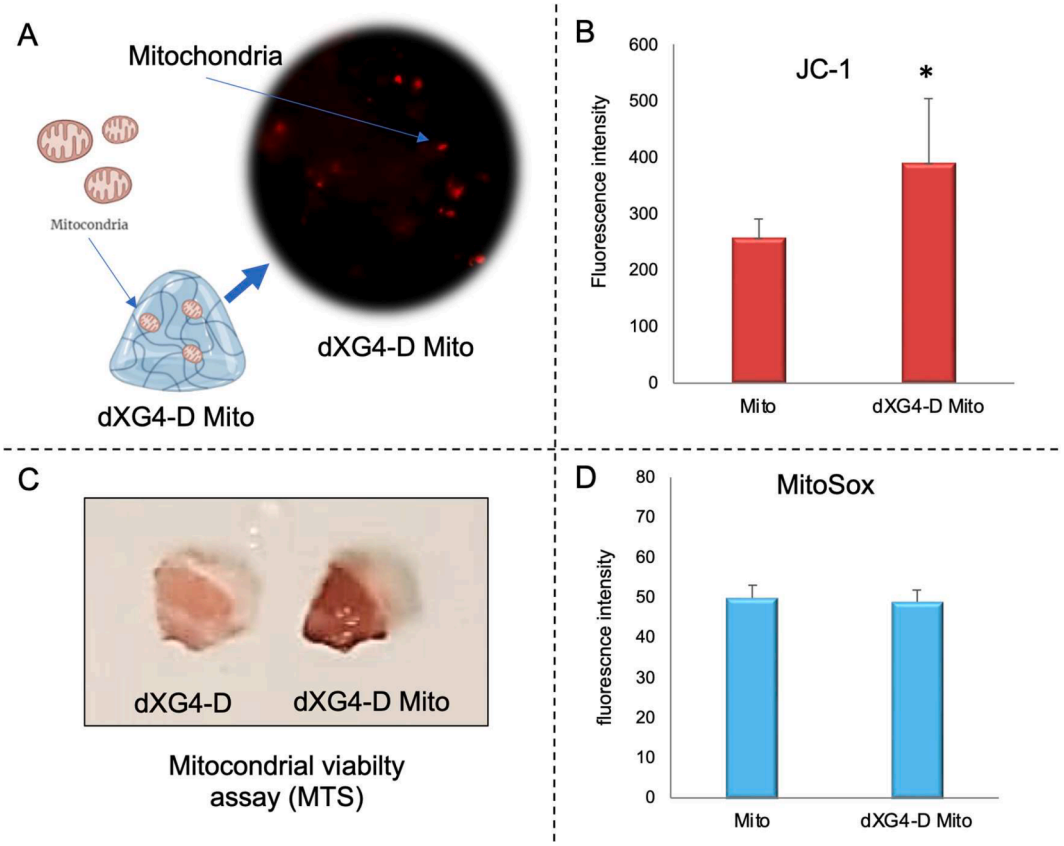

Fig. 4. Characterization of mitochondria loaded in the hydrogel. (A) Fluorescence image of the JC-1-labeled mitochondria loaded in the hydrogel and (B) histogram of the relative intensity of the fluorescence levels of the free and loaded mitochondria in the hydrogel, indicative of mitochondrial health. (C) MTS assay (measurement of mitochondrial metabolic activity) image of the mitochondria-loaded hydrogel. (D) MitoSox assay histogram of the free and hydrogel-loaded mitochondria, indicating mitochondrial oxidative state. The results indicate that the mitochondria incorporated in the hydrogel are viable, healthy and metabolically active.

(Fig. 4A). Fluorescence microscopy analysis revealed mitochondrial red fluorescence inside the hydrogel, indicating that the hydrogel does not affect mitochondrial membrane potential (Fig. 4A). Furthermore, no adverse effects induced by the hydrogel were detected after 24 h of incubation (Fig. 4B). In particular, the presence of dXG4-D would seem to improve the level of mitochondrial membrane potential with respect to the one of free mitochondria, that is an indication of the state of good health of the hydrogel-incorporated mitochondria. This effect could be due to the ability of xyloglucan to improve energy metabolism (Lim & Lee, 2017). To confirm these results, mitochondria within the hydrogel were subjected to an MTS test. The hydrogel containing mitochondria has a brown color, indicating the presence of vital and metabolically active mitochondria (Fig. 4C). Moreover, the MitoSOX fluorescence probe was used to measure the superoxide species generated in mitochondria following alterations in their oxidative state. Mitochondria inside the gel showed the same fluorescence intensity levels as the free mitochondria, indicating that the hydrogel did not induce mitochondrial oxidative stress (Fig. 4D).

Oxidative stress can compromise the viability of exogenous mitochondria injected into damaged tissues. Therefore, we investigated whether mitochondria loaded in dXG4-D, compared to isolated mitochondria, retained their function after incubation with various concentrations of hydrogen peroxide (H_2O_2). After 1 and 24 h from the treatment, both the mitochondria loaded into the hydrogel and the free mitochondria were analyzed using JC-1. The hydrogel preserves the function of mitochondria at the concentration of 10 mM H_2O_2, a concentration able to induce serious organelle failure (Ikeda et al., 2021), while free mitochondria were affected by the oxidative stress (Fig. 5). Oxidative stress in extracellular environments can impair the viability of exogenous mitochondria during the MT process. Moreover, the level of oxidative stress and the concentration of H_2O_2 increase in pathological condition (Sies & Jones, 2020). Some authors have demonstrated that a system, such as mitochondria-rich extracellular vesicles, is necessary to protect the MT process from oxidative stress (Ikeda et al., 2021). The data reported in Fig. 5 suggest that mitochondria loaded into dXG4-D are more resistant to oxidative stress than free mitochondria.

3.4. Release of mitochondria from the hydrogel and cellular uptake

Several Fluorescent dyes are used to visualize intercellular transplanted mitochondria (Roushandeh et al., 2019). Since JC-1 does not fluoresce red in aqueous solutions and becomes red fluorescent after aggregating within living mitochondria, these properties make it suitable for use in release assays (Picone et al., 2021). The JC-1-labeled mitochondria were loaded into the gel, inserted into the apical transwell chamber, and kept at 37 °C up to 24 h (Fig. 6A). To test the release from the dXG4-D, the fluorescence in the medium of the basal chamber was measured at different times (1, 2, 4, 6, 20, 24 and 27 h). As shown in the histogram, the release started after 4 h, and continued up to more than 1 day (Fig. 6B). The sustained release of mitochondria, combined with their localization in the site of action, can ensure a gradual uptake by the target cells.

To perform the hydrogel-mediated delivery of mitochondria to the cells, mitochondria were isolated from SY-5YSH and, immediately prior to being loaded into the hydrogel, were labeled with the JC-1 Red probe. Then, the hydrogel loaded with mitochondria was inserted into the apical chamber of the transwell where NIH 3T3 cells had previously seeded in the basolateral chamber (Fig. 6C). After 24 h, the presence of red fluorescence in the cells was visualized and monitored by fluorescence microscopy (Fig. 6D). The dotted red fluorescence inside the cells demonstrates that the transfer of the mitochondria, released from the hydrogel and taken up by the cells, successfully occurred (Fig. 6D).

The transfer of mitochondria from the hydrogel to the cells was also confirmed by repeating the experiment with the mitochondria-laden hydrogel in the same culture plate of the cells. After 24 h it can be observed that several mitochondria are inside the cells, while some others are still in the hydrogel (Fig. 7).

Patel and co-workers developed an erodible thermogelling hydrogel for localized delivery of viable mitochondria in vivo. They found that mitochondria are released from the hydrogel within 20 min at 37 °C. Mitochondria are too large to diffuse through the gel network and are released following erosion of the hydrogel, with complete erosion occurring within 60 min (Patel et al., 2022). Similarly, the release profile shown in Fig. 6 is probably due to changes in the gel structure that can be observed through SEM analysis. The gradual increase in hydrogel pores observed, at 6 h and 24 h (Fig. 3B), due to rearrangement of the network in the release medium, can explain the sustained release of mitochondria.

3.5. Injectability

Shear viscosity measurements as a function of shear rate were performed to characterize the flow properties of the dXG dispersions mixed with DMEM and mitochondria. The measurements were carried out on systems freshly mixed with the media and compared to the analogous systems without mitochondria. The flow curves, reported in Fig. 8A, show the typical features of pseudo-plastic fluids. The viscosity decreases with the increase of the shear rate, as a result of the decrease in a number of entanglements when chains align parallel to the flow direction. The presence of mitochondria in the formulation does not significantly affect the apparent viscosity.

The results of this study align with previous findings that have examined the rheological properties and injectability of hydrogel systems for biomedical applications. For instance, the shear-thinning behavior observed in dXG dispersions, consistent with the flow properties of other polysaccharide-based hydrogels, facilitates injection (Yan et al., 2010). Moreover, the finding that the presence of mitochondria does not significantly alter the viscosity of the hydrogel is supported by

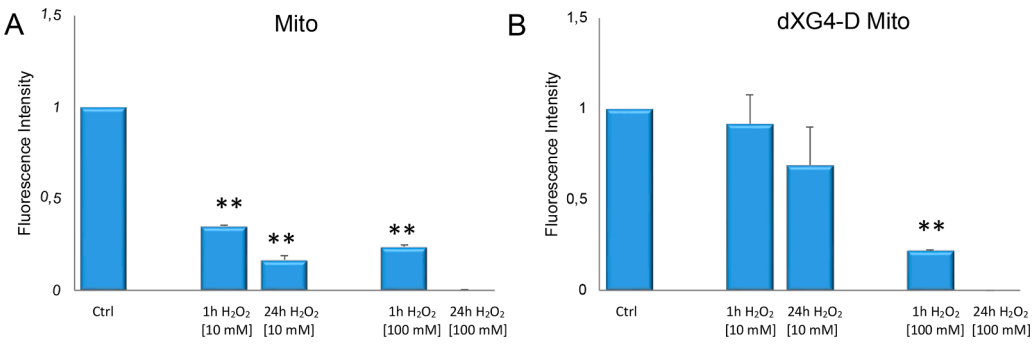

Fig. 5. Mitochondria within the hydrogel are more resistant to oxidative stress than isolated mitochondria. (A) Histogram of the JC-1 test of free mitochondria treated with H_2O_2 at different doses (10 and 100 mM) after 1 and 24 h. (B) JC-1 assay histogram of mitochondria loaded in the hydrogel treated with H_2O_2 at different doses (10 and 100 mM) for 1 and 24 h. The results indicate that the hydrogel is able to protect mitochondria from oxidative stress.

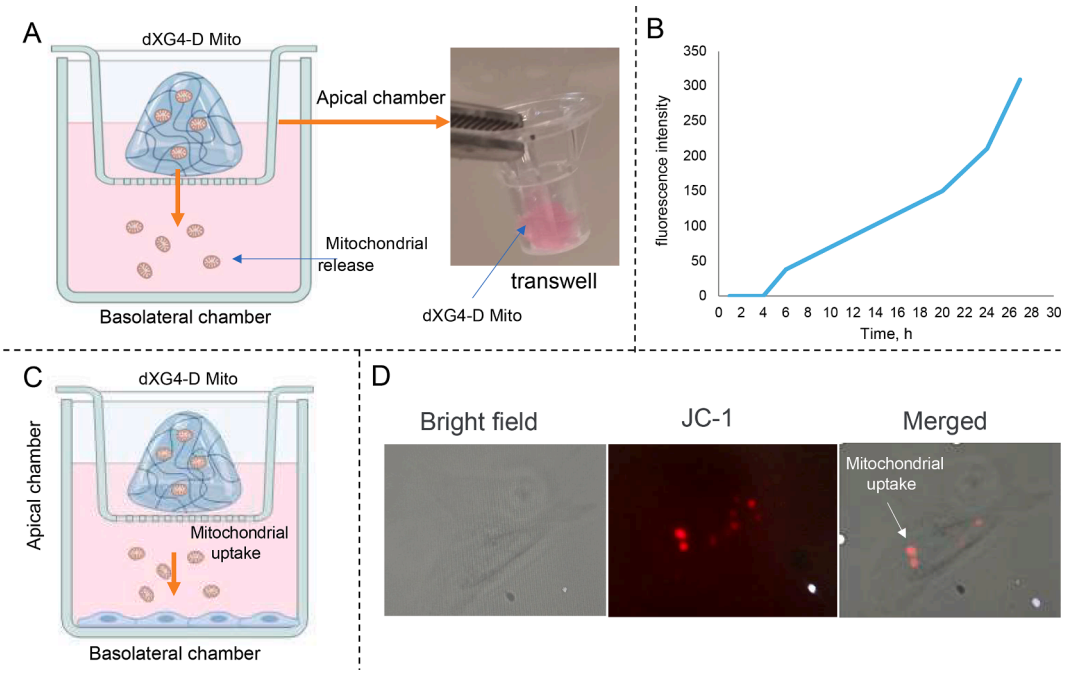

Fig. 6. Release of mitochondria from the hydrogel and cellular uptake. (A) Schematic representation of the transwell experiment to test mitochondrial release from the hydrogel. (B) Graph of the release profile of JC-1-labeled mitochondria from the hydrogel. (C) Schematic representation of the transwell experiment to test the release of JC-1-labeled mitochondria from the hydrogel to the cells and (D) related cell fluorescence image. The results indicate that mitochondria are released from the hydrogel and transferred to the cells.

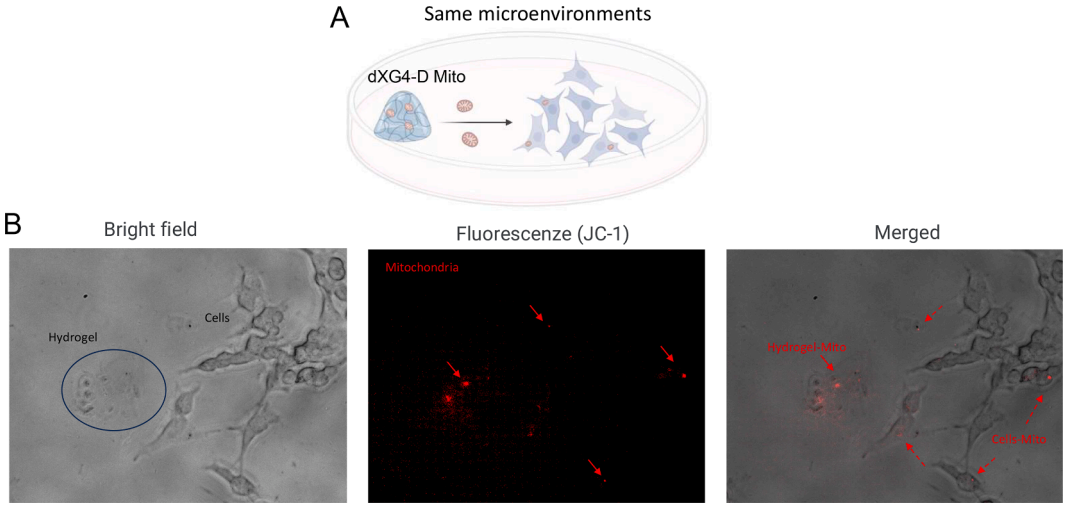

Fig. 7. Release and cellular uptake of the hydrogel loaded with mitochondria and cells in the same microenvironment. (A) Schematic representation of the experiment procedure. (B) Microscopy image of the hydrogel and cells (bright field), mitochondria label with JC-1 (fluorescence JC-1) and relative merged.

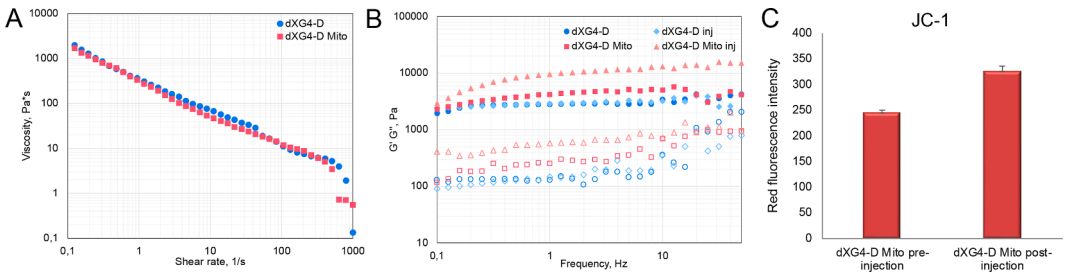

Fig. 8. Injectability evaluation. A) Shear viscosity of dXG4-D with and without mitochondria (Mito) as a function of the shear rate. B) Storage modulus, G' (full dot) and loss modulus, G'' (hollow dot) as a function of the frequency, for dXG4-D and dXG4-D Mito, before and after injection (inj). (C) Histogram of the fluorescence intensity of JC-1 test of mitochondria before and after injection.

similar studies where the incorporation of biological entities, like cells or nanoparticles, into hydrogel matrices did not drastically change their rheological properties (Y. Li et al., 2012; Muscolino et al., 2021; Toia et al., 2020).

In order to assess the effect of the injection on the hydrogel structure, the mixtures with or without mitochondria were injected directly on the rheometer plate through a G18 syringe needle and subjected to frequency sweep measurements and compared to the same systems not injected. The systems with and without mitochondria resulted perfectly injectable by a common operator while the G' and G" curves are shown in Fig. 8B. The mechanical spectra do not evidence any significant effect of the injection in hydrogel without mitochondria and an increase of the frequency-dependence of G' and of G" values for the mitochondria-laden hydrogels. The injectability and structural integrity of the hydrogel post-injection are crucial for its practical application in tissue engineering. The lack of significant changes in mechanical spectra post-injection for hydrogel without mitochondria, and the increase in frequency-dependence of G' and G" for mitochondria-laden hydrogels, suggests that the hydrogel matrix can withstand the mechanical stresses of injection without substantial degradation. This is comparable to findings in other studies where hydrogels were tested for injectability and mechanical integrity under similar conditions (Guvendiren et al., 2012).

With the idea of developing an injectable system containing the hydrogel to protect the mitochondria and deliver them through injection in a controlled environment, we analyzed whether the mechanical force exerted during the injection of the system, by using a syringe, could damage the mitochondria. For this purpose, pre- and post-injection JC1 tests were performed, and the data obtained (Fig. 8C) showed not only that there is no reduction in mitochondrial membrane potential before and after injection, but on the contrary, there is an increase, implying the absence of adverse effects during the injection process.

Studies have shown that external mechanical stimulation of intracellular or isolated mitochondria increases fission or fusion events (Phuyal et al., 2023). A theoretical approach highlighted that the mechanical parameters of the inner mitochondrial membrane, such as surface tension, bending stiffness, and elastic modulus of Gaussian curvature, are influenced by metabolic changes in the proton motive force and mitochondrial membrane potential (Chvanov, 2006). We cannot exclude that the force imparted to the mitochondria-laden hydrogels, during passage through the syringe, which results in an increase in the frequency-dependence of G' and of G" values, may induce an increase in the mitochondrial membrane potential.

Finally, in order to test the distribution of the hydrogel in the myocardium tissue, *ex-vivo* injection into the myocardial wall of swine hearts, purchased at the local food market, was tested as shown in Fig. 9. The injection of dXG 4 % % w gel into myocardial wall of swine heart with a G18 needle was smooth. The injected solution formed spheroidal gel particles in the myocardial wall without diffusing, as shown in photographs B and C taken after an incision on the left ventricle made after 6 h of incubation at 37 °C. This is a significant result considering the importance of controlled hydrogel distribution for effective tissue regeneration (Revete et al., 2022). These results are promising, not only considering that tamarind-derived xyloglucan showed myocardial protection by inhibiting apoptosis and improving energy metabolism (Lim & Lee, 2017), but also considering a possible function of the gel as a filler of the myocardium wall to contrast myocardial remodeling following acute infarction. Indeed, thinning of the infarcted region but also of the remote myocardium and ventricular dilation of the cavity adversely affect the long-term outcome after infarction. The dXG myocardial protection and potential to act as a myocardial wall filler to counteract

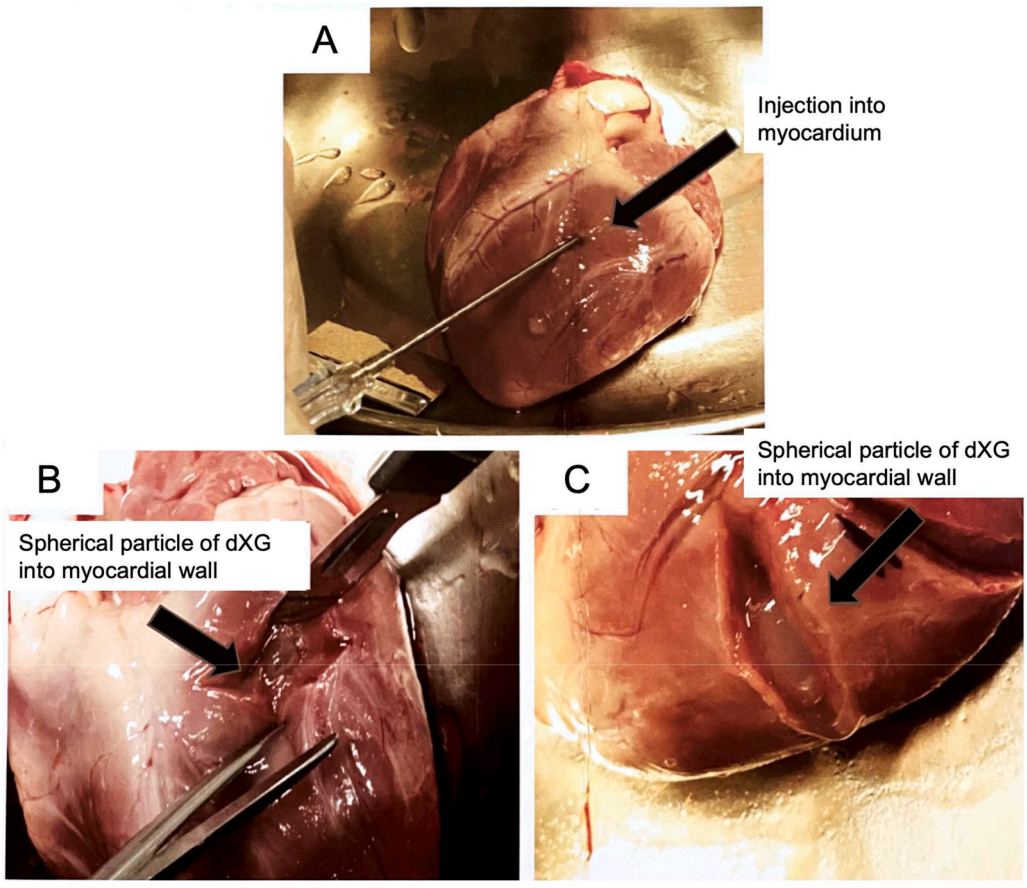

Fig. 9. Swine heart injection. (A) Photograph of a representative injection of dXG gel within the myocardial wall of a swine heart in a heated chamber kept at 37 °C; (B, C) Visual inspection after 24 h incubation and incision, showing the hydrogel spherical particle in the ventricular wall.

remodeling after infarction, as suggested by our results, are supported by studies showing similar benefits of hydrogel-based therapies in cardiac tissue engineering (P. Li et al., 2023).

4. Conclusions

This work aimed to demonstrate a possible use of a partially degalactosylated xyloglucan-based hydrogel as a sustained release device for mitochondria transplantation strategies to enhance myocardial regeneration after infarction. Our findings confirmed that dXG is biocompatible, injectable and forming gels rapidly at body temperature without cross-linking agents protecting mitochondria from oxidative stress, making it suitable for the scope of the study. MTS and JC-1 assays indicate that the mitochondria incorporated in the hydrogel are viable and metabolically active, also after being subjected to the shear forces of an injection with a G18 syringe needle. Mitosox assay results demonstrate that the hydrogel does not induce oxidative stress to the mitochondria but actually protects them from the oxidative stress that could be present in the affected portion of the left ventricle after a heart failure.

Release tests and inspections of the hydrogel microstructure suggest that the incorporated mitochondria are released slowly, probably due to the slow increase in pore size of the hydrogel matrix over time. The mitochondria were successfully internalized by cells after release. The injection of small volumes of aqueous dXG into the heart wall, formed well-defined hydrogel spheres which will prevent the uncontrolled dispersion of the mitochondria and allow the restoration of the geometry of the heart wall, thus limiting extensive ventricular dilatation improving cardiac function, with a minimally invasive intervention compared to the use of cardiac patches.

In light of these promising results, future studies will focus on the in vivo evaluation of this approach in animal models of heart failure. Additionally, long-term safety and potential side effects such as immune response will be evaluated. If the preclinical data were to be successful, we could hypothesize the clinical trial of a hydrogel implanted in the heart muscle via injection (non-invasive administration) which could improve cardiac functions in pathological conditions through the release of mitochondria.

Should they be successful, and should the results be confirmed in clinical trials, these or similar devices would establish a new paradigm in the treatment or management of debilitating cardiovascular diseases.

Ethical approval

The swine heart was purchased at the market so it does not need an ethics approval, according to our regulations.

Funding sources

Pasquale Picone and Domenico Nuzzo were funded by “Invecchiamento FOE 2022_DSB.AD006.371″, National Research Council - CNR, and Clelia Dispenza by the “Sicilian MicronanoTech Research And Innovation Center” - SAMOTHRACE – (B73C22000810001 - ECS_00000022) Spoke 3, and Emanuela Muscolino has received funding from the European Union - NextGenerationEU through the Italian Ministry of University and Research under PNRR - M4C2-I1.3 Project PE_00000019 "HEAL ITALIA" CUP B73C22001250006. The views and opinions expressed are those of the authors only and do not necessarily reflect those of the European Union or the European Commission. Neither the European Union nor the European Commission can be held responsible for them.

CRediT authorship contribution statement

Pasquale Picone: Investigation, Data curation, Methodology, Conceptualization, Validation, Project administration, Visualization, Writing – original draft, Funding acquisition, Resources. **Emanuela Muscolino:** Investigation, Data curation, Methodology, Conceptualization, Validation, Project administration, Visualization, Writing – original draft. **Antonella Girgenti:** Investigation, Data curation. **Maria Testa:** Investigation, Data curation. **Daniela Giacomazza:** Supervision. **Clelia Dispenza:** Supervision, Writing – review & editing, Funding acquisition, Resources. **Domenico Nuzzo:** Supervision, Writing – review & editing, Funding acquisition, Resources.

Declaration of competing interest

The authors declare that they have no known competing financial interests or personal relationships that could have appeared to influence the work reported in this paper.

Data availability

Data will be made available on request.

Acknowledgments

We wish to acknowledge Dr. Akira Tabuchi and Mr. Masanori Miyakoshi of MP GOKYO FOOD & CHEMICAL CO., LTD. for supplying the biopolymer used for this work.

Supplementary materials

Supplementary material associated with this article can be found, in the online version, at doi:10.1016/j.carpta.2024.100543.

References

Belosludtsev, K. N., Belosludtseva, N. V., & Dubinin, M. V. (2020). Diabetes mellitus, mitochondrial dysfunction and Ca2+-dependent permeability transition pore. *International Journal of Molecular Sciences, 21*(18), 6559. https://doi.org/10.3390/ijms21186559

Bertero, E., Maack, C., & O'Rourke, B (2018). Mitochondrial transplantation in humans: “Magical” cure or cause for concern? *Journal of Clinical Investigation, 128*(12), 5191–5194. https://doi.org/10.1172/JCI124944

Bonafede, R., & Mariotti, R. (2017). ALS pathogenesis and therapeutic approaches: The role of mesenchymal stem cells and extracellular vesicles. *Frontiers in Cellular Neuroscience, 11*, 80. https://doi.org/10.3389/fncel.2017.00080

Bragoszewski, P., Turek, M., & Chacinska, A. (2017). Control of mitochondrial biogenesis and function by the ubiquitin-proteasome system. *Open Biology, 7*(4), Article 170007. https://doi.org/10.1098/rsob.170007

Cha, M.-Y., Han, S.-H., Son, S. M., Hong, H.-S., Choi, Y.-J., Byun, J., & Mook-Jung, I. (2012). Mitochondria-Specific accumulation of amyloid β induces mitochondrial dysfunction leading to apoptotic cell death. *PLoS ONE, 7*(4), e34929. https://doi.org/10.1371/journal.pone.0034929

Chen, D., Guo, P., Chen, S., Cao, Y., Ji, W., Lei, X., Liu, L., Zhao, P., Wang, R., Qi, C., Liu, Y., & He, H. (2012). Properties of xyloglucan hydrogel as the biomedical sustained-release carriers. *Journal of Materials Science: Materials in Medicine, 23*(4), 955–962. https://doi.org/10.1007/s10856-012-4564-z

Chen, X., Ji, Y., Liu, R., Zhu, X., Wang, K., Yang, X., Liu, B., Gao, Z., Huang, Y., Shen, Y., Liu, H., & Sun, H. (2023). Mitochondrial dysfunction: Roles in skeletal muscle atrophy. *Journal of Translational Medicine, 21*(1), 503. https://doi.org/10.1186/s12967-023-04369-z

Chvanov, M. (2006). Metabolic control of elastic properties of the inner mitochondrial membrane. *The Journal of Physical Chemistry. B, 110*(45), 22903–22909. https://doi.org/10.1021/jp0638181

Dea, I. C. M. (1989). Industrial polysaccharides. *Pure and Applied Chemistry, 61*(7), 1315–1322. https://doi.org/10.1351/pac198961071315

Di Carlo, M., Giacomazza, D., Picone, P., Nuzzo, D., & San Biagio, P. L. (2012). Are oxidative stress and mitochondrial dysfunction the key players in the neurodegenerative diseases? *Free Radical Research, 46*(11), 1327–1338. https://doi.org/10.3109/10715762.2012.714466

Dispenza, C., Todaro, S., Bulone, D., Sabatino, M. A., Ghersi, G., San Biagio, P. L., & Lo Presti, C. (2017). Physico-Chemical and mechanical characterization of in-situ forming xyloglucan gels incorporating a growth factor to promote cartilage reconstruction. *Materials Science and Engineering: C, 70*, 745–752. https://doi.org/10.1016/j.msec.2016.09.045

Ditta, L. A., Bulone, D., Biagio, P. L. S., Marino, R., Giacomazza, D., & Lapasin, R. (2020). The degree of compactness of the incipient high methoxyl pectin networks. A rheological insight at the sol-gel transition. *International Journal of Biological Macromolecules, 158*, 985–993. https://doi.org/10.1016/j.ijbiomac.2020.05.019

Dutta, P., Giri, S., & Giri, T. K. (2020). Xyloglucan as green renewable biopolymer used in drug delivery and tissue engineering. *International Journal of Biological Macromolecules, 160*, 55–68. https://doi.org/10.1016/j.ijbiomac.2020.05.148

Emani, S. M., Piekarski, B. L., Harrild, D., Del Nido, P. J., & McCully, J. D. (2017). Autologous mitochondrial transplantation for dysfunction after ischemia-reperfusion injury. *The Journal of Thoracic and Cardiovascular Surgery, 154*(1), 286–289. https://doi.org/10.1016/j.jtcvs.2017.02.018

Giacomazza, D., Bulone, D., San Biagio, P. L., Marino, R., & Lapasin, R. (2018). The role of sucrose concentration in self-assembly kinetics of high methoxyl pectin. *International Journal of Biological Macromolecules, 112*, 1183–1190. https://doi.org/10.1016/j.ijbiomac.2018.02.103

Giannoccaro, M. P., La Morgia, C., Rizzo, G., & Carelli, V. (2017). Mitochondrial DNA and primary mitochondrial dysfunction in Parkinson's disease. *Movement Disorders: Official Journal of the Movement Disorder Society, 32*(3), 346–363. https://doi.org/10.1002/mds.26966

Gollihue, J. L., Patel, S. P., Eldahan, K. C., Cox, D. H., Donahue, R. R., Taylor, B. K., Sullivan, P. G., & Rabchevsky, A. G. (2018). Effects of mitochondrial transplantation on bioenergetics, cellular incorporation, and functional recovery after spinal cord injury. *Journal of Neurotrauma, 35*(15), 1800–1818. https://doi.org/10.1089/neu.2017.5605

Gollihue, J. L., Patel, S. P., Mashburn, C., Eldahan, K. C., Sullivan, P. G., & Rabchevsky, A. G. (2017). Optimization of mitochondrial isolation techniques for intraspinal transplantation procedures. *Journal of Neuroscience Methods, 287*, 1–12. https://doi.org/10.1016/j.jneumeth.2017.05.023

Guvendiren, M., Lu, H. D., & Burdick, J. A. (2012). Shear-thinning hydrogels for biomedical applications. *Soft Matter, 8*(2), 260–272. https://doi.org/10.1039/C1SM06513K

Han, M., Liu, Y., Zhang, F., Sun, D., & Jiang, J. (2020). Effect of galactose side-chain on the self-assembly of Xyloglucan macromolecule. *Carbohydrate Polymers, 246*, Article 116577. https://doi.org/10.1016/j.carbpol.2020.116577

Ikeda, G., Santoso, M. R., Tada, Y., Li, A. M., Vaskova, E., Jung, J.-H., O'Brien, C., Egan, E., Ye, J., & Yang, P. C. (2021). Mitochondria-Rich extracellular vesicles from autologous stem cell-derived cardiomyocytes restore energetics of ischemic myocardium. *Journal of the American College of Cardiology, 77*(8), 1073–1088. https://doi.org/10.1016/j.jacc.2020.12.060

Kaza, A. K., Wamala, I., Friehs, I., Kuebler, J. D., Rathod, R. H., Berra, I., Ericsson, M., Yao, R., Thedsanamoorthy, J. K., Zurakowski, D., Levitsky, S., Del Nido, P. J., Cowan, D. B., & McCully, J. D. (2017). Myocardial rescue with autologous mitochondrial transplantation in a porcine model of ischemia/reperfusion. *The Journal of Thoracic and Cardiovascular Surgery, 153*(4), 934–943. https://doi.org/10.1016/j.jtcvs.2016.10.077

Kuo, C.-C., Su, H.-L., Chang, T.-L., Chiang, C.-Y., Sheu, M.-L., Cheng, F.-C., Chen, C.-J., Sheehan, J., & Pan, H.-C. (2017). Prevention of axonal degeneration by perineurium injection of mitochondria in a sciatic nerve crush injury model. *Neurosurgery, 80*(3), 475–488. https://doi.org/10.1093/neuros/nyw090

Lea, P. J., & Hollenberg, M. J. (1989). Mitochondrial structure revealed by high-resolution scanning electron microscopy. *American Journal of Anatomy, 184*(3), 245–257. https://doi.org/10.1002/aja.1001840308

Li, P., Hu, J., Wang, J., Zhang, J., Wang, L., & Zhang, C. (2023). The role of hydrogel in cardiac repair and regeneration for myocardial infarction: recent advances and future perspectives. *Bioengineering, 10*(2), 165. https://doi.org/10.3390/bioengineering10020165

Li, Y., Rodrigues, J., & Tomás, H. (2012). Injectable and biodegradable hydrogels: Gelation, biodegradation and biomedical applications. *Chemical Society Reviews, 41*(6), 2193–2221. https://doi.org/10.1039/C1CS15203C

Lim, S. H., & Lee, J. (2017). Xyloglucan intake attenuates myocardial injury by inhibiting apoptosis and improving energy metabolism in a rat model of myocardial infarction. *Nutrition Research, 45*, 19–29. https://doi.org/10.1016/j.nutres.2017.07.003

Lin, L., Xu, H., Bishawi, M., Feng, F., Samy, K., Truskey, G., Barbas, A. S., Kirk, A. D., & Brennan, T. V. (2019). Circulating mitochondria in organ donors promote allograft rejection. *American Journal of Transplantation, 19*(7), 1917–1929. https://doi.org/10.1111/ajt.15309

Loureiro, R., Mesquita, K. A., Magalhães-Novais, S., Oliveira, P. J., & Vega-Naredo, I. (2017). Mitochondrial biology in cancer stem cells. *Seminars in Cancer Biology, 47*, 18–28. https://doi.org/10.1016/j.semcancer.2017.06.012

Lu, J., Zheng, X., Li, F., Yu, Y., Chen, Z., Liu, Z., Wang, Z., Xu, H., & Yang, W. (2017). Tunneling nanotubes promote intercellular mitochondria transfer followed by increased invasiveness in bladder cancer cells. *Oncotarget, 8*(9), 15539–15552. https://doi.org/10.18632/oncotarget.14695

Ma, X., McKeen, T., Zhang, J., & Ding, W.-X. (2020). Role and mechanisms of mitophagy in liver diseases. *Cells, 9*(4), 837. https://doi.org/10.3390/cells9040837

Masuzawa, A., Black, K. M., Pacak, C. A., Ericsson, M., Barnett, R. J., Drumm, C., Seth, P., Bloch, D. B., Levitsky, S., Cowan, D. B., & McCully, J. D. (2013). Transplantation of autologously derived mitochondria protects the heart from ischemia-reperfusion injury. *American Journal of Physiology-Heart and Circulatory Physiology, 304*(7), H966–H982. https://doi.org/10.1152/ajpheart.00883.2012

McCully, J. D., Cowan, D. B., Emani, S. M., & Del Nido, P. J (2017). Mitochondrial transplantation: From animal models to clinical use in humans. *Mitochondrion, 34*, 127–134. https://doi.org/10.1016/j.mito.2017.03.004

McCully, J. D., Levitsky, S., Del Nido, P. J., & Cowan, D. B. (2016). Mitochondrial transplantation for therapeutic use. *Clinical and Translational Medicine, 5*(1), 16. https://doi.org/10.1186/s40169-016-0095-4

Miyazaki, S., Kawasaki, N., Kubo, W., Endo, K., & Attwood, D. (2001). Comparison of in situ gelling formulations for the oral delivery of cimetidine. *International Journal of Pharmaceutics, 220*(1–2), 161–168. https://doi.org/10.1016/S0378-5173(01)00669-X

Muscolino, E., Di Stefano, A. B., Trapani, M., Sabatino, M. A., Giacomazza, D., Moschella, F., Cordova, A., Toia, F., & Dispenza, C. (2021). Injectable xyloglucan hydrogels incorporating spheroids of adipose stem cells for bone and cartilage regeneration. *Materials Science and Engineering: C, 131*, Article 112545. https://doi.org/10.1016/j.msec.2021.112545

Muscolino, E., Sabatino, M. A., Jonsson, M., & Dispenza, C. (2024). The role of water in radiation-induced fragmentation of cellulosic backbone polysaccharides. *Cellulose, 31*(2), 841–856. https://doi.org/10.1007/s10570-023-05660-4

Paliwal, S., Chaudhuri, R., Agrawal, A., & Mohanty, S. (2018). Regenerative abilities of mesenchymal stem cells through mitochondrial transfer. *Journal of Biomedical Science, 25*(1), 31. https://doi.org/10.1186/s12929-018-0429-1

Patel, S. P., Michael, F. M., Arif Khan, M., Duggan, B., Wyse, S., Darby, D. R., Chaudhuri, K., Pham, J. T., Gollihue, J., DeRouchey, J. E., Sullivan, P. G., Dziubla, T. D., & Rabchevsky, A. G. (2022). Erodible thermogelling hydrogels for localized mitochondrial transplantation to the spinal cord. *Mitochondrion, 64*, 145–155. https://doi.org/10.1016/j.mito.2022.04.002

Pecora, D., Annunziata, F., Pegurri, S., Picone, P., Pinto, A., Nuzzo, D., & Tamborini, L. (2022). Flow synthesis of nature-inspired mitochondria-targeted phenolic derivatives as potential neuroprotective agents. *Antioxidants, 11*(11), 2160. https://doi.org/10.3390/antiox11112160

Phuyal, S., Romani, P., Dupont, S., & Farhan, H. (2023). Mechanobiology of organelles: Illuminating their roles in mechanosensing and mechanotransduction. *Trends in Cell Biology, 33*(12), 1049–1061. https://doi.org/10.1016/j.tcb.2023.05.001

Picone, P., & Nuzzo, D. (2022). Promising treatment for multiple sclerosis: Mitochondrial transplantation. *International Journal of Molecular Sciences, 23*(4), 2245. https://doi.org/10.3390/ijms23042245

Picone, P., Nuzzo, D., Caruana, L., Scafidi, V., & Di Carlo, M. (2014). Mitochondrial dysfunction: Different routes to Alzheimer's disease therapy. *Oxidative Medicine and Cellular Longevity, 2014*, Article 780179. https://doi.org/10.1155/2014/780179

Picone, P., Nuzzo, D., Giacomazza, D., & Di Carlo, M. (2020). β-Amyloid peptide: The cell compartment multi-faceted interaction in Alzheimer's disease. *Neurotoxicity Research, 37*(2), 250–263. https://doi.org/10.1007/s12640-019-00116-9

Picone, P., Porcelli, G., Bavisotto, C. C., Nuzzo, D., Galizzi, G., Biagio, P. L. S., Bulone, D., & Di Carlo, M. (2021). Synaptosomes: New vesicles for neuronal mitochondrial transplantation. *Journal of Nanobiotechnology, 19*(1), 6. https://doi.org/10.1186/s12951-020-00748-6

Picone, P., Vilasi, S., Librizzi, F., Contardi, M., Nuzzo, D., Caruana, L., Baldassano, S., Amato, A., Mulè, F., San Biagio, P. L., Giacomazza, D., & Di Carlo, M. (2016). Biological and biophysics aspects of metformin-induced effects: Cortex mitochondrial dysfunction and promotion of toxic amyloid pre-fibrillar aggregates. *Aging, 8*(8), 1718–1734. https://doi.org/10.18632/aging.101004

Poznyak, A. V., Ivanova, E. A., Sobenin, I. A., Yet, S.-F., & Orekhov, A. N. (2020). The role of mitochondria in cardiovascular diseases. *Biology, 9*(6), 137. https://doi.org/10.3390/biology9060137

Preble, J. M., Pacak, C. A., Kondo, H., MacKay, A. A., Cowan, D. B., & McCully, J. D. (2014). Rapid isolation and purification of mitochondria for transplantation by tissue dissociation and differential filtration. *Journal of Visualized Experiments, 91*, 51682. https://doi.org/10.3791/51682

Protasoni, M., & Zeviani, M. (2021). Mitochondrial structure and bioenergetics in normal and disease conditions. *International Journal of Molecular Sciences, 22*(2), 586. https://doi.org/10.3390/ijms22020586

Ramirez-Barbieri, G., Moskowitzova, K., Shin, B., Blitzer, D., Orfany, A., Guariento, A., Iken, K., Friehs, I., Zurakowski, D., Del Nido, P. J., & McCully, J. D. (2019). Alloreactivity and allorecognition of syngeneic and allogeneic mitochondria. *Mitochondrion, 46*, 103–115. https://doi.org/10.1016/j.mito.2018.03.002

Revete, A., Aparicio, A., Cisterna, B. A., Revete, J., Luis, L., Ibarra, E., Segura González, E. A., Molino, J., & Reginensi, D. (2022). Advancements in the use of hydrogels for regenerative medicine: Properties and biomedical applications. *International Journal of Biomaterials, 2022*, 1–16. https://doi.org/10.1155/2022/3606765

Roushandeh, A. M., Kuwahara, Y., & Roudkenar, M. H. (2019). Mitochondrial transplantation as a potential and novel master key for treatment of various incurable diseases. *Cytotechnology, 71*(2), 647–663. https://doi.org/10.1007/s10616-019-00302-9

Rüb, C., Wilkening, A., & Voos, W. (2017). Mitochondrial quality control by the Pink1/Parkin system. *Cell and Tissue Research, 367*(1), 111–123. https://doi.org/10.1007/s00441-016-2485-8

Sakakibara, C. N., Sierakowski, M. R., Chassenieux, C., Nicolai, T., & De Freitas, R. A. (2017). Xyloglucan gelation induced by enzymatic degalactosylation; kinetics and the effect of the molar mass. *Carbohydrate Polymers, 174*, 517–523. https://doi.org/10.1016/j.carbpol.2017.06.118

Salimi, A., Roudkenar, M. H., Sadeghi, L., Mohseni, A., Seydi, E., Pirahmadi, N., & Pourahmad, J. (2015). Ellagic acid, a polyphenolic compound, selectively induces ROS-mediated apoptosis in cancerous B-lymphocytes of CLL patients by directly targeting mitochondria. *Redox Biology, 6*, 461–471. https://doi.org/10.1016/j.redox.2015.08.021

Salimi, A., Roudkenar, M. H., Seydi, E., Sadeghi, L., Mohseni, A., Pirahmadi, N., & Pourahmad, J. (2017). Chrysin as an anti-cancer agent exerts selective toxicity by directly inhibiting mitochondrial complex II and V in CLL B-lymphocytes. *Cancer Investigation, 35*(3), 174–186. https://doi.org/10.1080/07357907.2016.1276187

Shaki, F., Shayeste, Y., Karami, M., Akbari, E., Rezaei, M., & Ataee, R. (2017). The effect of epicatechin on oxidative stress and mitochondrial damage induced by homocycteine using isolated rat hippocampus mitochondria. *Research in Pharmaceutical Sciences, 12*(2), 119. https://doi.org/10.4103/1735-5362.202450

Shi, X., Zhao, M., Fu, C., & Fu, A. (2017). Intravenous administration of mitochondria for treating experimental Parkinson's disease. *Mitochondrion, 34*, 91–100. https://doi.org/10.1016/j.mito.2017.02.005

Shirakawa, M., Yamatoya, K., & Nishinari, K. (1998). Tailoring of xyloglucan properties using an enzyme. *Food Hydrocolloids, 12*(1), 25–28. https://doi.org/10.1016/S0268-005X(98)00052-6

Sies, H., & Jones, D. P. (2020). Reactive oxygen species (ROS) as pleiotropic physiological signalling agents. *Nature Reviews Molecular Cell Biology, 21*(7), 363–383. https://doi.org/10.1038/s41580-020-0230-3

Todaro, S., Dispenza, C., Sabatino, M. A., Ortore, M. G., Passantino, R., San Biagio, P. L., & Bulone, D. (2015). Temperature-induced self-assembly of degalactosylated xyloglucan at low concentration. *Journal of Polymer Science Part B: Polymer Physics, 53*(24), 1727–1735. https://doi.org/10.1002/polb.23895

Todaro, S., Sabatino, M. A., Mangione, M. R., Picone, P., Di Giacinto, M. L., Bulone, D., & Dispenza, C. (2016). Temporal control of xyloglucan self-assembly into layered structures by radiation-induced degradation. *Carbohydrate Polymers, 152*, 382–390. https://doi.org/10.1016/j.carbpol.2016.07.005

Toia, F., Di Stefano, A. B., Muscolino, E., Sabatino, M. A., Giacomazza, D., Moschella, F., Cordova, A., & Dispenza, C. (2020). In-situ gelling xyloglucan formulations as 3D artificial niche for adipose stem cell spheroids. *International Journal of Biological Macromolecules, 165*, 2886–2899. https://doi.org/10.1016/j.ijbiomac.2020.10.158

Wang, S.-F., Chen, S., Tseng, L.-M., & Lee, H.-C. (2020). Role of the mitochondrial stress response in human cancer progression. *Experimental Biology and Medicine, 245*(10), 861–878. https://doi.org/10.1177/1535370220920558

Wu, S., Zhang, A., Li, S., Chatterjee, S., Qi, R., Segura-Ibarra, V., Ferrari, M., Gupte, A., Blanco, E., & Hamilton, D. J. (2018). Polymer functionalization of isolated mitochondria for cellular transplantation and metabolic phenotype alteration. *Advanced Science, 5*(3), Article 1700530. https://doi.org/10.1002/advs.201700530

Yan, C., Altunbas, A., Yucel, T., Nagarkar, R. P., Schneider, J. P., & Pochan, D. J. (2010). Injectable solid hydrogel: Mechanism of shear-thinning and immediate recovery of injectable β-hairpin peptide hydrogels. *Soft Matter, 6*(20), 5143. https://doi.org/10.1039/c0sm00642d

Zhang, H.-Y., Lü, N.-H., Xie, Y., Guo, G.-H., Zhan, J.-H., & Chen, J. (2008). Influence of heat shock preconditioning on structure and function of mitochondria in gastric mucosa of severely burned animals: Experiment with rats. *Zhonghua Yi Xue Za Zhi, 88*(8), 564–567.

Zhao, J., Wang, X., Huo, Z., Chen, Y., Liu, J., Zhao, Z., Meng, F., Su, Q., Bao, W., Zhang, L., Wen, S., Wang, X., Liu, H., & Zhou, S. (2022). The impact of mitochondrial dysfunction in amyotrophic lateral sclerosis. *Cells, 11*(13), 2049. https://doi.org/10.3390/cells11132049